

## pH Regulation of Connexin43: Molecular Analysis of the Gating Particle

José F. Ek-Vitorín,\* Guillermo Calero,\* Gregory E. Morley,\* Wanda Coombs,\* Steven M. Taffet,# and Mario Delmar\*

Departments of \*Pharmacology, and #Microbiology and Immunology, SUNY/Health Science Center at Syracuse, Syracuse, New York 13210 USA

**ABSTRACT** Gap junction channels allow for the passage of ions and small molecules between neighboring cells. These channels are formed by multimers of an integral membrane protein named connexin. In the heart and other tissues, the most abundant connexin is a 43-kDa, 382-amino acid protein termed connexin43 (Cx43). A characteristic property of connexin channels is that they close upon acidification of the intracellular space. Previous studies have shown that truncation of the carboxyl terminal of Cx43 impairs pH sensitivity. In the present study, we have used a combination of optical, electrophysiological, and molecular biological techniques and the oocyte expression system to further localize the regions of the carboxyl terminal that are involved in pH regulation of Cx43 channels. Our results show that regions 261–300 and 374–382 are essential components of a pH-dependent “gating particle,” which is responsible for acidification-induced uncoupling of Cx43-expressing cells. Regions 261–300 and 374–382 seem to be interdependent. The function of region 261–300 may be related to the presence of a poly-proline repeat between amino acids 274 and 285. Furthermore, site-directed mutagenesis studies show that the function of region 374–382 is not directly related to its net balance of charges, although mutation of only one amino acid (aspartate 379) for asparagine impairs pH sensitivity to the same extent as truncation of the carboxyl terminal domain (from amino acid 257). The mutation in which serine 364 is substituted for proline, which has been associated with some cases of cardiac congenital malformations in humans, also disrupts the pH gating of Cx43, although deletion of amino acids 364–373 has no effect on acidification-induced uncoupling. These results provide new insight into the molecular mechanisms responsible for acidification-induced uncoupling of gap junction channels in the heart and in other Cx43-expressing structures.

### INTRODUCTION

The synchronization of cellular function within a tissue is regulated in part by the existence of low-resistance intercellular channels called gap junctions. Selected ions and intracellular messengers diffuse from cell to cell across these channels, thereby coordinating the activity of individual cells to bring about the synchronous response of an entire organ (Kanno et al., 1995).

Gap junctions are found in most tissues of vertebrate and invertebrate species across phylogenetic distances (Bennett et al., 1995). Gap junction channels are formed by multimers of a membrane protein named connexin (Bennett and Verselis, 1992; Kumar and Gilula, 1992). Six connexin subunits form a hexameric structure called a connexon. Two connexons, each provided by one cell in the pair, assemble to form a gap junction channel. A number of connexin proteins have been identified (Bennett et al., 1995; Dahl et al., 1995); information available from hydropathy analyses and antibody, protease, and mutagenesis studies indicate a highly conserved membrane topology for all connexins studied: four transmembrane domains, two extracellular loops, one intracellular loop, and both the amino and carboxyl termini located in the cytoplasm (Stauffer and Unwin, 1992; Bennett et al., 1991).

Recently, a number of investigators have applied site-directed mutagenesis techniques to correlate changes in the primary sequence of a given connexin with certain functions. Some of those studies have led to the localization and predicted secondary structure of the regions of connexin involved in the binding of two connexons (Rosinski and Nicholson, 1994; Dahl et al., 1992). Others have focused on the structural bases for voltage gating (Suchyna et al., 1993), and yet others have investigated the molecular determinants controlling the compatibility between connexins (Bruzzone et al., 1994).

We have used site-directed mutagenesis techniques to characterize the regions of Cx43 that are involved in acidification-induced uncoupling (i.e., pH gating). Our studies have shown that pH gating of Cx43-expressing oocytes can be altered by truncation of the carboxyl terminal region (Liu et al., 1993; Morley et al., 1996), or by mutations of the histidine residue located at position 95 (Ek et al., 1994). Moreover, we have demonstrated that coexpression of the carboxyl terminal restores the pH sensitivity of a mutant lacking such a structure (Morley et al., 1996). Our previous results (Liu et al., 1993; Morley et al., 1996) have shown that the carboxyl terminal is an independent domain that is essential for the pH gating of Cx43 at intracellular pH (pH<sub>i</sub>) values between 7.2 and 6.2. Based on such data, we have proposed that pH gating of Cx43 results from a protein-protein interaction (either direct, or mediated by an intermediary molecule) between the carboxyl terminal domain, which acts as a particle, and a separate region of the con-

Received for publication 4 October 1995 in final form 22 May 1996.

Address reprint requests to Dr. Mario Delmar, Department of Pharmacology, SUNY/Health Science Center, 766 Irving Avenue, Syracuse NY 13210. Tel.: 315-464-7987; Fax: 315-464-8014; E-mail: delmarM@vax.cs.hscsyr.edu.

© 1996 by the Biophysical Society

0006-3495/96/09/1273/12 \$2.00

nexin molecule, which acts as a receptor for that particle (Delmar et al., 1994; Morley et al., 1996).

The aim of the present study was to localize more specifically the regions of the carboxyl terminal that are involved in pH regulation of Cx43 channels. We have identified two particular regions: one is included within residues 261–300, and the other within the last nine amino acids of the sequence (374–382). Coexpression studies show that deletion of these two regions prevents the carboxyl terminal from acting as a pH-dependent binding particle. Amino acid substitution studies suggest that the conformation of the carboxyl terminal end, and not only net balances of charge, are involved in the interactions of the carboxyl terminal particle with the region of connexin that acts as the receptor. These data constitute the first step toward characterizing the specific particle-receptor interactions that underlie acidification-induced uncoupling of oocyte pairs expressing Cx43.

## MATERIALS AND METHODS

### Oocyte preparation and recording

Experiments were carried out using antisense-injected pairs of *Xenopus* oocytes expressing mRNA for Cx43 or its mutants. The preparation of oocytes has been detailed elsewhere (Liu et al., 1993; Ek et al., 1994). Briefly, Stage V or VI oocytes (Dumont, 1972) were obtained from adult female *Xenopus laevis* frogs. The cells were mechanically stripped of their follicular layer, collagenase-treated, and then injected with antisense for the endogenous connexin (Cx38; see Barrio et al., 1991). Three to five days after antisense injection, the cells were injected with mRNA for wild-type or mutant Cx43. Approximately 24 h after mRNA injection, the cells were mechanically stripped of their vitelline layer and paired by the vegetal poles. After 6 to 9 h of pairing, each cell was voltage clamped using the conventional two-electrode voltage clamp configuration (Spray et al., 1981). Expression of functional connexins was detected by measuring the flow of electrical current from one cell to the other, and junctional conductance ( $G_j$ ) was estimated from the amplitude of the junctional current divided by the voltage gradient across the junction (Spray et al., 1981).

For the experiments described in Figs. 2–7, where a one-step acidification protocol was used (Ek et al., 1994), the bathing solution used during electrophysiological recordings contained (in mM) Na-acetate, 102; NaCl, 20; KCl, 1.0; NaHCO<sub>3</sub>, 2.4; MgSO<sub>4</sub>, 0.82; CaCl<sub>2</sub>, 0.74; HEPES, 15; the pH of the solution was adjusted (with 0.1 N HCl or 0.1 N NaOH) to either 7.4 (in control) or 6.2 (during acidification). The specifics of the acidification protocol have been detailed elsewhere (Ek et al., 1994) and are further defined in the Results. For the experiments outlined in Figs. 8–11, where intracellular pH was determined simultaneously with the changes in electrical coupling (Morley et al., 1996), acidification was induced by superfusing the oocytes with a saline solution gassed with progressively increasing concentrations of CO<sub>2</sub> (Morley et al., 1996). The composition of the superfusate used for these experiments was (in mM) NaCl, 88; KCl, 1; MgSO<sub>4</sub>, 0.82; CaCl<sub>2</sub>, 0.74; NaHCO<sub>3</sub>, 18.

### Site-directed mutagenesis

Site-directed mutagenesis was carried out following the technique of Vandeyar et al. (1988), as detailed elsewhere (Ek et al., 1994). Throughout this paper, deletion mutants are indicated by the sign D, followed by the location of the first amino acid deleted and the location of the last amino acid that is missing from the sequence. Truncation mutants are noted by the letter M followed by the number of the last amino acid in the sequence. Substitutions are denoted by the one-letter code name of the amino acid being replaced, followed by the number of that residue in the Cx43

sequence and the one-letter code name of the amino acid used to replace it. When more than one residue has been substituted, the substitutions are listed in sequence, separated by a hyphen (e.g., D378N-D379N-E381Q) or a slash ( $\Delta$ 281–300/M374). The numbers that locate the amino acid positions were based on the primary sequence published by Beyer et al. (1987). For convenient reference, the amino acid sequence of the carboxyl terminal of rat cardiac Cx43 is presented in Fig. 1. All mutations tested (with the exception of mutant S364P) are listed in Table 1. mRNA coding for both the mutant and wild-type carboxyl terminal domains was prepared by polymerase chain reaction, using either intact or mutated cDNA clones as the templates (see Morley et al., 1996, for further details).

### Western blotting

For Western immunoblot detection of mutant and wild-type carboxyl terminal peptides, groups of four oocytes were lysed in a solution of 1% NP40, 50 mM iodoacetamide, 1 mM phenylmethanesulphonyl fluoride, 1 mM EDTA, 1  $\mu$ M leupeptin, 2  $\mu$ g/ml aprotinin, and 0.7  $\mu$ g/ml pepstatin in borate buffer at pH 8.0 (Goldberg and Lau, 1993). The lysate was clarified by centrifugation and resolved on a 15% polyacrylamide gel. The proteins were transferred to nitrocellulose and analyzed for Cx43 peptides. Membranes were blocked overnight at room temperature in Tween-TBS (TTBS) (20 mM Tris-HCl, pH 7.5; 500 mM NaCl; 0.1% Tween-20; 0.02% sodium azide) containing 10% nonfat milk powder (blocking solution). The membranes were then incubated using a 1:1000 dilution of anti-Cx43 serum (Zymed Laboratories, South San Francisco, CA) in blocking solution at room temperature for 2 h followed by extensive washing in TTBS. Blots were then incubated with a 1:3000 dilution of goat anti-rabbit IgG-peroxidase (Boehringer Mannheim, Indianapolis, IN) in blocking solution followed by washing with TTBS. Antigen was detected using the enhanced chemiluminescence Western blotting detection system (Amersham Corp., Arlington Heights, IL).

### Simultaneous measurements of pH<sub>i</sub> and G<sub>j</sub>

For the experiments presented in Figs. 8–11, acidification-induced uncoupling was correlated with pH<sub>i</sub>. Intracellular pH was measured by detecting the light emission of the proton-sensitive fluorophore seminaaphthorhodafluor (SNARF; dextran form), as previously described (Morley et al., 1996). Briefly, oocytes were injected with 50 nl of a concentrated (0.357 mM) dye solution. Optical recordings were obtained using either a SPEX Fluorolog system (Morley et al., 1996) or a RatioMaster system (Photon

```

221  L A L N I I E L F Y V F F K G V K D R V
241  K G R S D P Y H A T T G P L S P S K D C
261  G S P K Y A Y F N G C S S P T A P L S P
281  M S P P G Y K L V T G D R N N S S C R N
301  Y N K Q A S E Q N W A N Y S A E Q N R M
321  G Q A G S T I S N S H A Q P F D F P D D
341  N Q N A K K V A G H E L Q P L A I V D
361  O R P S S R A S S R A S S R P R P D D I E I

```

FIGURE 1 Amino acid sequence of the carboxyl terminal domain of rat cardiac connexin43 (Cx43). Amino acids are denoted using the one-letter code. The numbers at the left indicate the sequence position of the first amino acid on that line. Numbers are assigned per the system of Beyer et al. (1987).

**TABLE 1** Mutations tested

Transcript	$G_j$ control ( $\mu$ S)		$G_j$ max ( $\mu$ S)		$G_j$ min/ $G_j$ max		n
	Mean	SEM	Mean	SEM	Mean	SEM	
Cx43	10.6	2.0	12.1	1.9	0.149	0.014	20
$\Delta$ 241–260	6.7	1.7	7.2	1.7	0.122	0.015	10
$\Delta$ 301–320	11.5	2.7	12.9	2.7	0.257	0.067	8
$\Delta$ 321–340	8.8	2.5	11.6	3.0	0.353	0.102	8
$\Delta$ 341–360	13.0	2.1	16.5	1.9	0.333	0.099	8
* $\Delta$ 261–280	12.9	1.8	16.5	2.0	0.521	0.085	8
* $\Delta$ 281–300	10.4	2.8	15.1	3.3	0.525	0.094	9
* $\Delta$ 281–290	10.6	2.5	15.4	2.9	0.523	0.107	8
* $\Delta$ 291–300	11.3	2.3	17.9	2.9	0.520	0.089	9
*M361	5.1	1.1	14.7	3.0	0.479	0.063	12
*M374	6.3	2.1	10.9	3.5	0.417	0.084	9
$\Delta$ 364–373	16.1	2.5	19.2	2.8	0.210	0.033	8
*P277A–280A	10.5	1.8	16.1	2.3	0.549	0.082	9
*D378N–D379N–E381	10.3	2.5	16.7	3.4	0.917	0.046	8
*D379N	10.7	2.0	11.8	2.8	0.836	0.081	9
*D379Q	10.5	1.9	13.3	2.7	0.815	0.053	8
D379k	5.3	2.2	6.3	2.4	0.304	0.075	8
D378N–D379N	10.1	1.3	13.8	1.3	0.323	0.055	8
D379N–E381Q	4.6	1.1	5.7	1.1	0.158	0.009	8
D378N	12.1	2.1	15.7	2.2	0.332	0.081	9
E381Q	6.5	1.7	8.7	1.7	0.171	0.022	9
D378N–E381Q	6.0	1.1	7.5	1.3	0.093	0.015	8
*P375A–377A	7.2	2.0	12.7	1.7	0.583	0.103	8
*R374Q–R376Q	11.1	2.0	18.2	2.4	0.734	0.095	8

$G_j$  control, junctional conductance recorded in control solution, before acidification.  $G_j$  max, Maximum junctional conductance recorded during acidification. n, number of oocyte pairs tested. Nomenclature defining each mutant is described in the text. Asterisks indicate mutants with susceptibility to uncoupling statistically different from wild type. Details on statistical analysis can be found in the text.

Technology International) equipped for single excitation, dual emission. The oocytes were illuminated with a xenon arc lamp, at a wavelength of 534 nm. Emission was recorded at 590 nm and at 640 nm. To calibrate the RatioMaster system, dextran SNARF-injected oocytes were incubated in sodium acetate-containing solutions at various pH values; after recording of a dual-emission ratio, the oocytes were transported to the SPEX system, where a full-emission spectrum was recorded. The same oocyte was then returned to the RatioMaster system, and an additional emission ratio was recorded to ensure that it was consistent with the one recorded before the emission spectra. The SPEX emission spectra had in turn been calibrated against pH<sub>i</sub> using pH-sensitive microelectrodes (Morley et al., 1996; their figure 1). Junctional conductance was recorded simultaneously during acidification, and  $G_j$ -pH<sub>i</sub> curves were obtained by correlating the value of pH<sub>i</sub> with the measurement of  $G_j$  (relative to  $G_j$  max) at each point in time.

### Statistical analysis

Statistical comparisons were made by parametric, one-way analysis of variance, followed by a Bonferroni test. Unless otherwise indicated, all mutants were compared only against the wild-type protein. Susceptibility to uncoupling of a given mutant was deemed to be significantly different from that of the wild type if the corrected *p* value was lower than 0.05. Average data are reported as mean  $\pm$  SEM.

## RESULTS AND DISCUSSION

### Susceptibility to acidification-induced uncoupling of wild-type Cx43

We have used a standardized acidification protocol and site-directed mutagenesis to study the correlation between the primary structure of Cx43 and the susceptibility to

acidification-induced uncoupling. Fig. 2 serves to illustrate the experimental procedure. Fig. 2 A shows the time course of low pH-induced changes in  $G_j$  recorded from a pair of oocytes expressing wild-type Cx43 mRNA. Ordinates on the left indicate the absolute value of  $G_j$ , and the ordinates on the right show the value of junctional conductance relative to the maximum  $G_j$  ( $G_j$  max) recorded. The solid bar on the top indicates the onset and duration of superfusion of a sodium acetate-containing solution buffered at a pH of 6.2 (intracellular pH at steady state varied between 6.1 and 6.3; see Liu et al., 1993). The variables  $G_j$  min and  $G_j$  max correspond, respectively, to the minimum and maximum values of  $G_j$  recorded during the acidification process. Uncoupling was defined as a reduction of  $G_j$  to less than 20% of  $G_j$  max (i.e.,  $G_j$  min/ $G_j$  max < 0.2; see horizontal dotted line). The susceptibility to acidification-induced uncoupling was defined by the ratio  $G_j$  min/ $G_j$  max. In all experiments, washout of the acidic solution was initiated either when  $G_j$  dropped below 20% of  $G_j$  max, or after 40 min of superfusion with the low pH solution. The example presented in Fig. 2 A illustrates the characteristic pattern of uncoupling and washout of Cx43 pairs (Swenson et al., 1989; Werner et al., 1991; Ek et al., 1994; White et al., 1994). Experiments in which  $G_j$  did not recover upon washout were not included in this study.

Fig. 2 B shows the average time course of acidification-induced uncoupling, recorded from 20 oocyte pairs expressing wild-type Cx43. In this and other similar plots presented

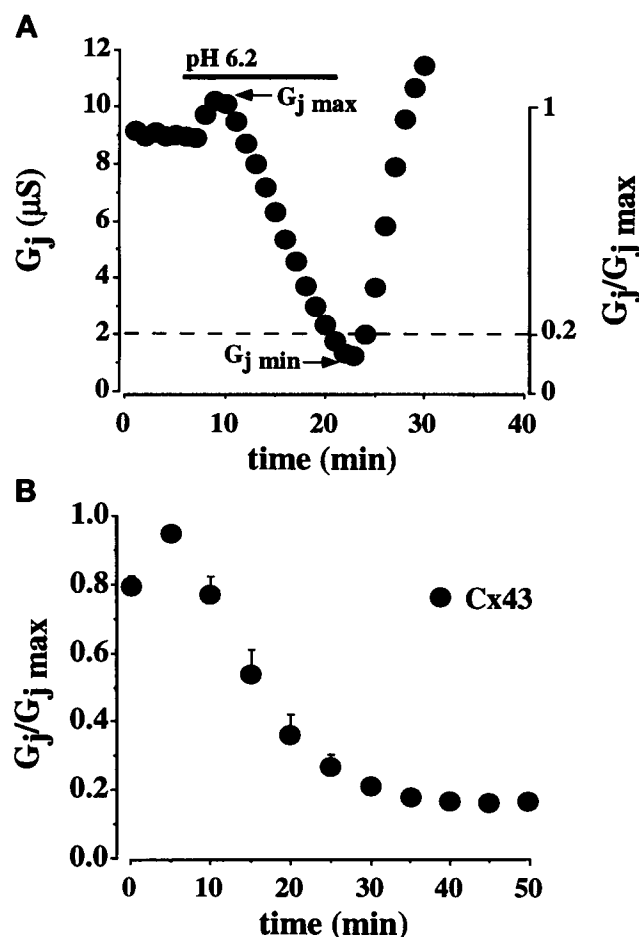


**FIGURE 2** Time course and extent of acidification-induced uncoupling of Cx43. (A) Data obtained from a Cx38-antisense-injected oocyte pair expressing wild-type Cx43. The horizontal bar at the top indicates the duration of superfusion with a sodium acetate-containing solution buffered at a pH of 6.2. Ordinates at the left indicate the absolute value of junctional conductance ( $G_j$ ), and the ordinates at the right correspond to the value of  $G_j$  relative to the maximum  $G_j$  recorded ( $G_{j\ max}$ ).  $G_{j\ min}$ , minimum value of  $G_j$  recorded during or immediately after acidification. Washout was initiated when the  $G_j/G_{j\ max}$  ratio was 0.2 (horizontal dotted line) or after 40 min of low pH superfusion. (B) Average time course of acidification-induced uncoupling of oocyte pairs injected with wild-type Cx43 mRNA. Data points are the mean value of 20 experiments; vertical bars correspond to standard error of the mean. Time 0 corresponds to the onset of low-pH superfusion.

in this paper, zero time corresponds to the onset of acidification. Average data points ( $\pm$  SEM) were calculated using either the magnitude of  $G_j/G_{j\ max}$  at a particular point in time or, if uncoupling had already occurred, with the corresponding  $G_{j\ min}/G_{j\ max}$  value. The curve shows the characteristic increase, followed by a rapid decrease (Swenson et al., 1989; Werner et al., 1991; Ek et al., 1994; White et al., 1994). The minimum value corresponds to the average  $G_{j\ min}/G_{j\ max}$  recorded from a particular group of experiments and thus reflects the susceptibility to acidification-induced uncoupling for that particular connexin.

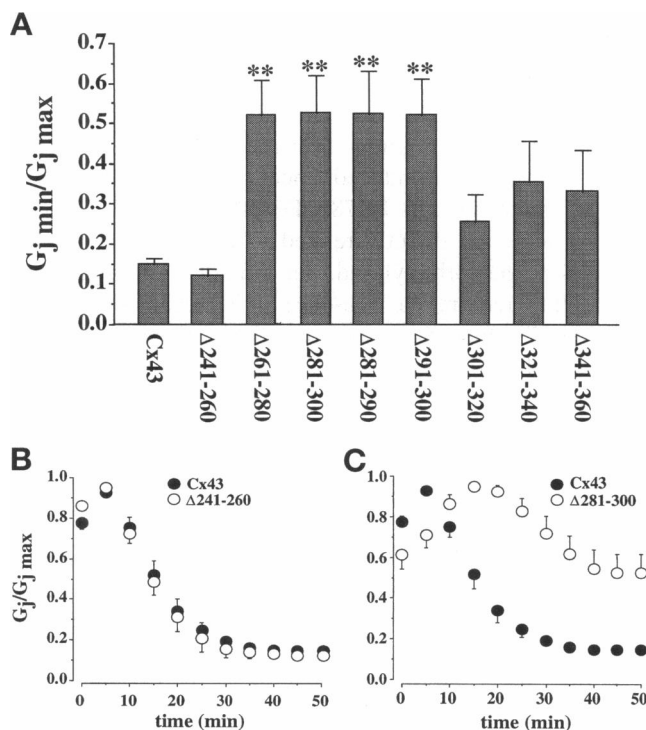
### Mutants tested and average $G_j$ values recorded

Table 1 provides a list of all the connexin mutants tested with the standardized acidification protocol. The table also summarizes the values for the control  $G_j$  and the  $G_{j\ max}$ , as well as for the susceptibility to acidification-induced uncoupling (i.e., ratio  $G_{j\ min}/G_{j\ max}$ ) measured from each connexin (mean  $\pm$  SEM). Only those experiments in which a complete acidification protocol (including washout) was carried out are included. Parametric one-way analysis of variance (followed by a Bonferoni test) showed no statistical differences between the average  $G_j$  values of any of the mutants when compared against wild-type.  $G_j$  values similar to those reported in this study have been used to compare the level of expression among connexins (White et al., 1995; Bruzzone et al., 1994; White et al., 1994) and to determine the pH sensitivity of Cx32 (Werner et al., 1991) and Cx43 (Werner et al., 1991; Liu et al., 1993) and their mutants (Ek et al., 1994). We did not find a correlation between the average  $G_j$  (either in control or at  $G_{j\ max}$ ) and the susceptibility to acidification-induced uncoupling of the various mutants.

### Deletion mutants: localization of regions relevant to pH gating of Cx43

As a first approach, we tested a series of deletion mutants to localize the regions of the carboxyl terminal of Cx43 that are important for pH regulation. Fig. 3 A shows the susceptibility to acidification-induced uncoupling (expressed as  $G_{j\ min}/G_{j\ max}$ ) of oocytes injected with wild-type or mutant Cx43 mRNA; Fig. 3, B and C, depicts the average time course of uncoupling for some of the mutants. The data show that deletion of amino acids 241–260, 301–320, 321–340, and 341–360 did not significantly affect the pH induced closure of Cx43. However, the susceptibility to acidification-induced uncoupling was significantly reduced (yet not completely prevented) after residues 261–280 or 281–300 were deleted from the sequence. Similar results were observed when only 10 amino acids (281–290 or 291–300) were deleted. The latter suggests that normal pH gating depends on the integrity of the 261–300 region. Moreover, the data show that the loss of pH sensitivity was not simply due to the shortening of the carboxyl terminal domain, because deletions of similar length in neighboring regions did not significantly affect the susceptibility to acidification-induced uncoupling.

The data presented on Fig. 4 show that truncation of the carboxyl terminal at amino acid 361 (M361) also impaired (although it did not completely prevent) pH-induced closure of Cx43 channels. Similar results were obtained when only the last nine amino acids were deleted from the sequence (mutant M374). However, deletion of segment 364–373, which contains a number of potential phosphorylation sites, did not affect pH gating of Cx43. These results do not support the previously postulated hypothesis (reviewed in



**FIGURE 3** (A) Average  $G_j \text{ min}/G_j \text{ max}$  ratios measured from oocyte pairs injected with the transcripts denoted at the bottom of each bar. Intracellular acidification was induced using the experimental protocol detailed in Fig. 2. Vertical bars correspond to the standard error of the mean for each group. Number of experiments for each series, as well as absolute values of control and maximum  $G_j$ , are presented in Table 1. All deletion mutants were grouped into one analysis of variance (corrected by a Bonferroni test) and compared against the wild-type protein. Statistical significance is denoted as follows: no asterisk,  $p > 0.05$ ; one asterisk (\*),  $p < 0.05$ ; two asterisks (\*\*),  $p < 0.01$ . (B and C) Average time course and extent of uncoupling of wild-type Cx43 (●) when compared to that of various mutants (○). Definitions of nomenclature can be found in Materials and Methods.

Delmar et al., 1994) that a change in the phosphorylation state of serine residues within the 364–373 region is an essential step in acidification-induced uncoupling of these channels.

#### Point mutations in region 261–300: possible role of prolines 277 and 280

Analysis of the primary structure of the 261–300 region shows a proline-rich sequence with a (PXX)<sub>4</sub> repeat (... PTAPLSPMSPPG...; residues 274–285). These sequences commonly present a characteristic secondary structure consisting of a stable, left-handed (type II)  $\alpha$ -helix with a full turn every three amino acids (Adzhubei and Sternberg, 1993; Williamson, 1994). Interestingly, polyproline II (PP II)  $\alpha$ -helices are often involved in protein-protein binding reactions (Adzhubei and Sternberg, 1993; Williamson, 1994; Cohen et al., 1995; Lins and Brasseur, 1995; Yu et al., 1994; Lim et al., 1994). Furthermore, serine residues within the 274–285 region

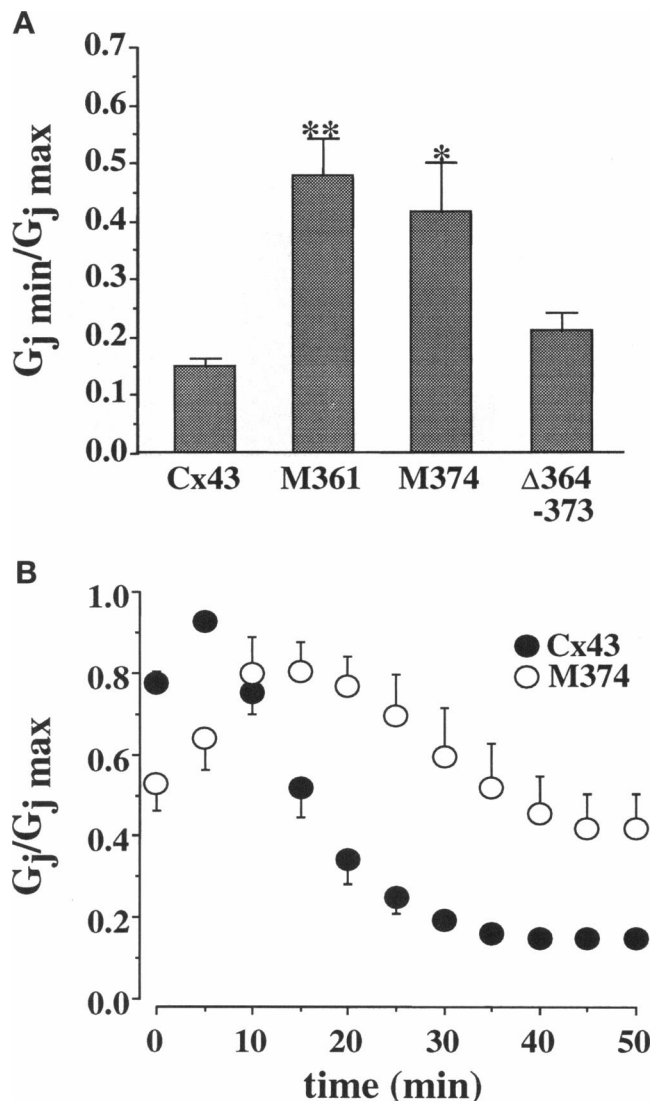


**FIGURE 4** Susceptibility to acidification-induced uncoupling of carboxyl-end mutants of Cx43. (A) Normalized average value of the minimum junctional conductance recorded during acidification ( $G_j \text{ min}/G_j \text{ max}$  ratio). Vertical bars correspond to SEM. Nomenclature defining the mutations is described in Materials and Methods. Statistical significance is denoted as follows: no asterisk,  $p > 0.05$ ; one asterisk (\*),  $p < 0.05$ ; two asterisks (\*\*),  $p < 0.01$ . (B) Time course of uncoupling of wild-type Cx43 (●) and of a truncation mutant in which amino acids 374–382 were deleted (M374; ○).

of Cx43 are known to be substrates for mitogen-activated protein kinase phosphorylation (Warn-Cramer et al., 1996). As an initial approach to studying the importance of the structural integrity of this region on the pH gating of Cx43, we determined the pH sensitivity of a mutant in which the prolines at positions 277 and 280 were replaced by alanines (mutant P277A-P280A). As shown in Fig. 5, such a mutation had an effect similar to that of deletion of the entire 261–300 region. We speculate that part of the secondary structure of region 261–300 may correspond to a PP II  $\alpha$ -helix, similar to that observed in

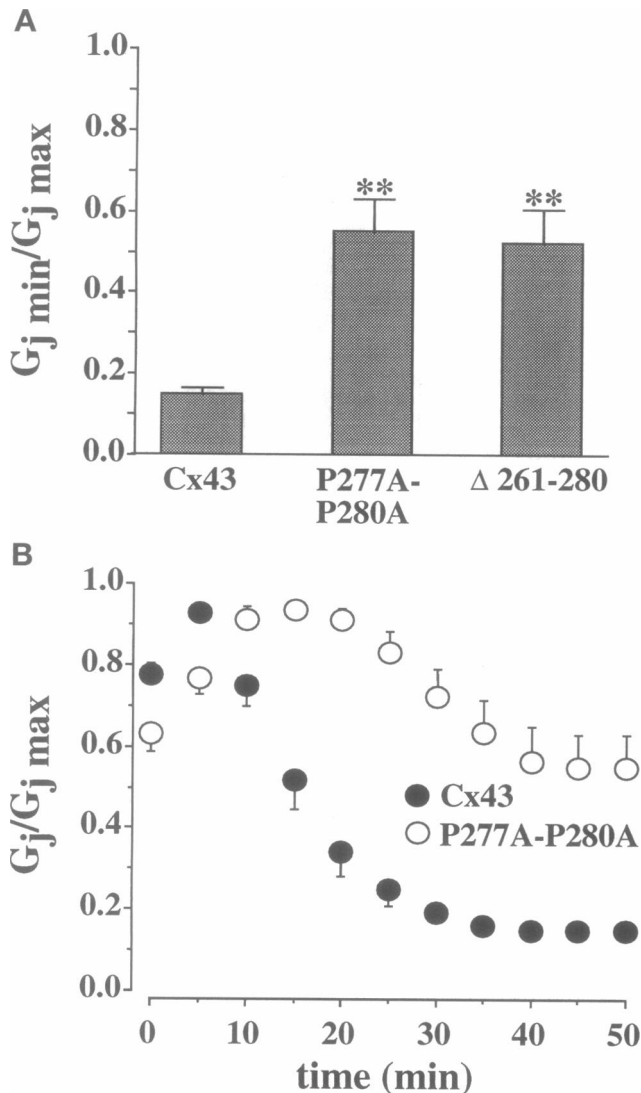


FIGURE 5 Susceptibility to acidification-induced uncoupling after mutation of prolines 277 and 280 for alanines (P277A-P280A). The two asterisks (\*\*) indicate  $p < 0.01$  when compared against wild type. The results were similar to those obtained after deletion 261–280 (mutant D261–280).

src-homology 3-binding proteins (Yu et al., 1994; Lim et al., 1994).

### Is pH gating related to the net balance of charges in the 374–382 region?

Previous studies on potassium channels have shown that the affinity between the voltage gating particle (the “ball” in the ball-and-chain model of voltage gating; see, e.g., Hoshi et al., 1990) and its receptor is a function of the net balance of charges within the particle (Toro et al., 1994). As a next step, we aimed to determine whether susceptibility to uncoupling was related to the net balance of charge in region 374–382. We used the one-step acidification protocol as a screening procedure to identify the relevant mutations. As

shown in Fig. 6, A and B, substitution of the acidic residues at the carboxyl end for their uncharged amide (mutant D378N-D379N-E381Q) significantly prevented pH gating. Single substitutions of aspartate 379 for either asparagine (mutant D379N) or glutamine (mutant D379Q) also prevented acidification-induced uncoupling. Yet, the results obtained with mutants D378N-D379N-E381Q, D379N, or D379Q were not directly related to the number of acidic residues at the carboxyl end, nor did acidification-induced uncoupling require the presence of a negative charge at position 379. Indeed, as shown in Fig. 6 C, normal uncoupling was found in cell pairs expressing a mutant in which aspartate 379 was replaced by a positively charged amino acid (mutant D379K). Furthermore, normal pH sensitivity was observed for D379N if an additional acidic residue was replaced by its amide (i.e., mutants D378N-D379N or D379N-E381Q). Finally, the susceptibility to acidification-induced uncoupling of mutants D378N and E381Q was similar to that of the wild-type protein, whereas the combined mutation D378N-E381Q seemed to enhance the pH sensitivity of Cx43 channels (see Fig. 6 D).

Further evidence that the function of the pH gating particle is not exclusively related to the net balance of charge in region 374–382 was obtained after substituting either the basic amino acids at positions 374 and 376 for polar residues (mutant R374Q-R376Q), or prolines 375 and 377 for alanines (mutant P375A-P377A). As shown in Fig. 7, these mutations had an effect similar to that of truncation of the entire 374–382 region. Yet, the net balance of charges was unaffected by the proline mutations. These results show a lack of correlation between the net balance of charge in region 374–382 and the susceptibility to acidification-induced uncoupling. The results are not surprising given the multiple ionic and nonionic interactions that may be expected to occur in such a highly charged, proline-rich region (Creighton, 1993; Lins and Brasseur, 1995). In such a complex environment, substitution of a particular amino acid could alter the balance of forces beyond what may be predicted by the simple algebraic addition of the charges of the basic and acidic residues involved.

An increase in  $G_j$  at the onset of acidification was apparent for most of the mutants, as well as for the wild-type protein. (Compare the values of  $G_j$  control against  $G_j \text{ max}$  in Table 1. See also Figs. 2–7 for examples.) An increase in  $G_j$  upon mild acidification has been reported by this (Liu et al., 1993; Ek et al., 1994; Morley et al., 1996) and other laboratories (e.g., Werner et al., 1991; Bennett et al., 1988; White et al., 1994), and it is thought to result from increased incorporation of functional channels (Werner et al., 1991). The molecular mechanisms responsible for this process are unknown, and its analysis goes beyond the scope of this project. However, it is interesting to note that pH-insensitive mutants such as D378N-D379N-E381Q may help in the study of this phenomenon, as they may allow us to dissociate the process of acidification-induced uncoupling from the increase in  $G_j$  that is observed as a result of mild acidification.

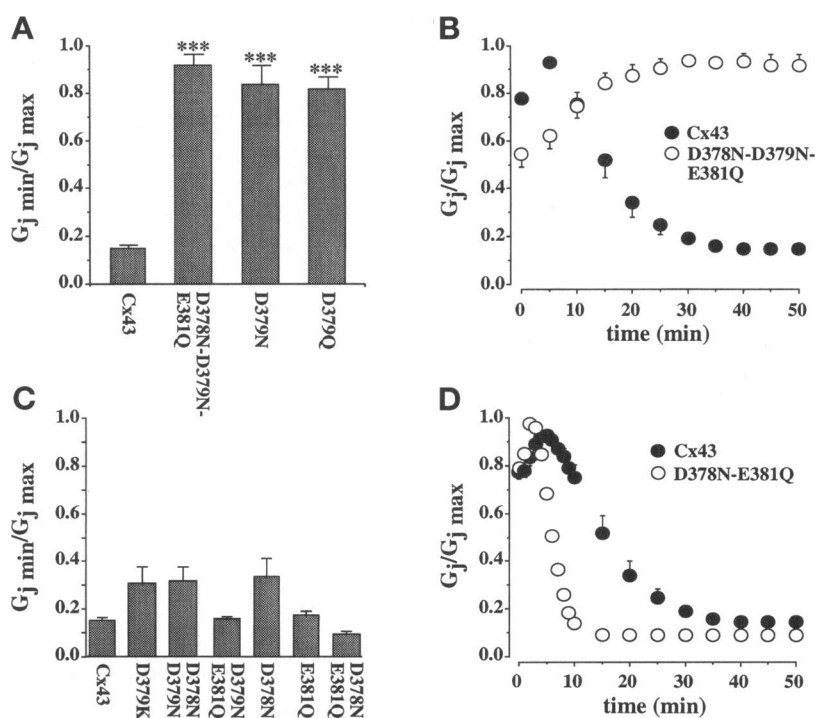


**FIGURE 6** (A and C) Susceptibility to acidification-induced uncoupling of Cx43 (expressed as  $G_j \text{ min}/G_j \text{ max}$  ratio) after mutation of the acidic residues at the carboxyl end. Same experimental protocol as described in Fig. 2. The nomenclature defining the specific mutations is explained in Materials and Methods. Number of experiments,  $G_j$  control, and  $G_j \text{ max}$  for each series are presented in Table 1. The  $G_j \text{ min}/G_j \text{ max}$  ratio obtained for each of the point mutations was compared against the wild-type protein using analysis of variance and a Bonferroni test. The three asterisks (\*\*\*) next to the bars for mutants D378N-D379N-E381Q, D379N, and D379Q indicate that the susceptibility to acidification-induced uncoupling for those mutants was significantly different ( $p < 0.001$ ) from wild type. None of the mutations presented in C caused significant changes in the susceptibility to acidification-induced uncoupling of Cx43. (B and D) Time course and extent of acidification-induced changes in  $G_j$  after substitution of the three acidic residues for their amides (B) or substitution of only D378 and E381 (D). The data show that mutation D378N-D379N-E381Q significantly impaired pH gating; leaving D379 intact while mutating the other two acidic residues seemed to enhance the development of acidification-induced uncoupling. In D, all data points collected within the first 10 min are displayed, so that the time course of uncoupling of mutant D378N-E381Q can be properly followed.

### Loss of pH sensitivity after deletions 281–300 and 361–382

To confirm that preservation of regions 261–300 and 361–382 was essential for normal pH gating, we determined the pH sensitivity of mutants  $\Delta 281$ –300 and M361. For the experiments described in this and the following sections, junctional conductance was measured simultaneously with intracellular pH; acidification was accomplished by progressively increasing the  $\text{CO}_2$  concentration in a bicarbonate-buffered solution. The plots presented on Fig. 8 were obtained by directly correlating  $G_j$  and  $\text{pH}_i$  at each point in time during acidification (see Materials and Methods; see also Morley et al., 1996). Data obtained from oocytes expressing wild-type Cx43 are presented in all panels for comparison (closed circles; continuous line). The control data were compiled from five previously published experiments (Morley et al., 1996) as well as from a new series of six control experiments performed with the RatioMaster system (see Materials and Methods). The control curve was fitted (least-squares convergence) with a Hill equation. Average  $\text{pK}_a$  (i.e., the  $\text{pH}_i$  that corresponds to a 50% decrease in  $G_j$ ) was  $6.73 \pm 0.067$ , and the average Hill coefficient

was  $4.85 \pm 0.304$  ( $n = 11$ ). Deletion of residues 281–300 (Fig. 8 A) significantly impaired pH gating. Truncation at amino acid 361 also impaired pH gating (Fig. 8 B). In this case, the average  $\text{pK}_a$  was  $6.61 \pm 0.01$  and the average Hill coefficient was  $5.5 \pm 0.45$  ( $n = 6$ ).

When the  $\text{CO}_2$  protocol was used, acidification of M361 to  $\text{pH}_i$  values below 6.4 caused  $G_j$  to decrease (in average) below 20% from  $G_j \text{ max}$  (Fig. 8 B). This is in contrast with the findings presented in Fig. 4, using the Na-acetate protocol. In that case, the average  $G_j$  of M361 only decreased to near 50% from  $G_j \text{ max}$  after acidification. We do not have a good explanation for this disparity. Yet it may be related to the different experimental protocols used. One of the things we have noticed when comparing results from the two different protocols is that the increase in conductance observed during acidification with Na-acetate is larger than the one recorded with the  $\text{CO}_2$  protocol. It is therefore possible that, when Na-acetate is used, the increase in  $G_j$  offsets the change in conductance due to closure of the channels. Alternatively, the extent of  $G_j$  change may be affected by the rate of acidification. In addition, the time course of pH gating of M361 may be slowed down as a

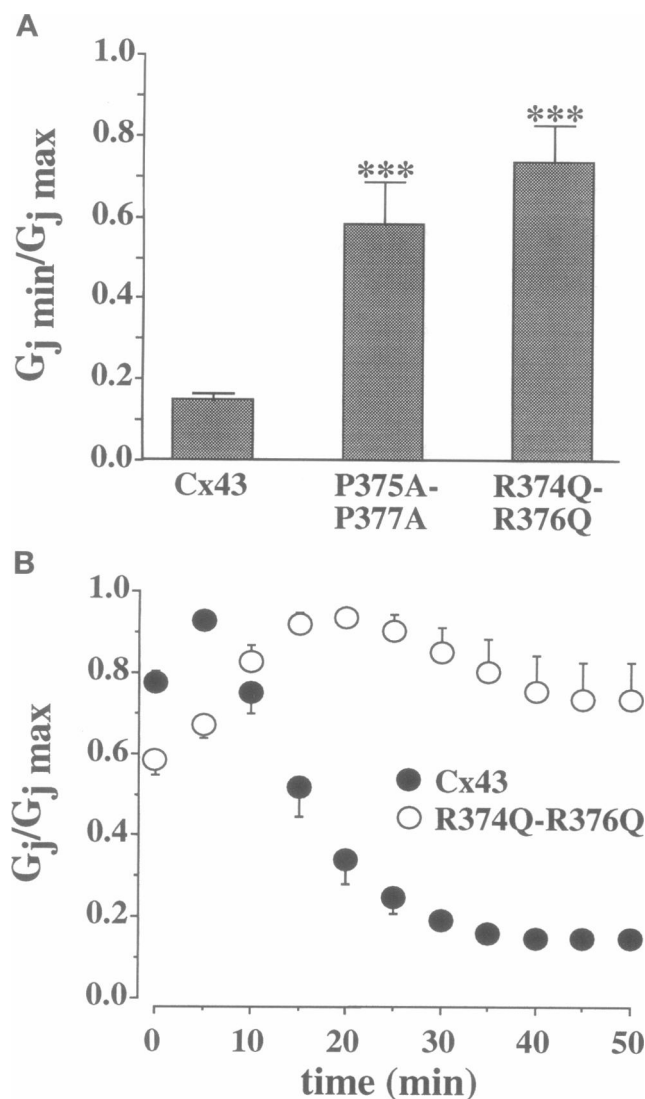


FIGURE 7 (A) Susceptibility to acidification-induced uncoupling after mutation of prolines 375 and 377 for alanines (P375A-P377A) or after replacing arginines 374 and 376 for glutamine (R374Q-R376Q; see also B). Both mutations caused a significant impairment of pH gating with respect to wild type (\*\*\*,  $p < 0.001$ ).

consequence of the mutation; in that case, the one-step acidification protocol may not allow enough time for channel closure before washout is started (even though superfusion of low pH solution is maintained for a total of 40 min). It is also possible that the control  $G_j$  when we use the bicarbonate buffer is different from that in the presence of Na-acetate, and that the extent of the uncoupling may be a function of the initial  $\text{pH}_i$ . Alternatively, the susceptibility to uncoupling may be dependent not only on the actual concentration of protons, but on the kind of buffer that is used. The idea that pH may affect  $G_j$  differently depending on the buffer used has been proposed previously (Pressler, 1989). In summary, it is clear that  $G_j$  increase is less apparent in those experiments where acidification is induced by progressively increasing the  $\text{CO}_2$  concentration in

a bicarbonate-buffered solution. It is also clear that the  $G_j$  of M361 decreases to a larger extent when the latter protocol is used. This protocol is the one used to obtain an actual correlation between  $G_j$  and  $\text{pH}_i$  values. The results stress the importance of using highly standardized experimental protocols for the study of pH gating of connexin channels.

The loss of pH sensitivity observed after truncation at amino acid 361 was most likely due to the absence of residues 374–382, because the pH sensitivity of a deletion mutant  $\Delta 364$ –373 was indistinguishable from that of the wild-type protein (Fig. 8 C). The average  $\text{pK}_a$  of this mutant was  $6.78 \pm 0.03$  and the Hill coefficient was  $5.36 \pm 0.86$  ( $n = 7$ ). These results are consistent with those observed using the one-step acidification protocol. In addition, they provide a quantitative analysis of the actual pH sensitivity of mutants that were less susceptible to acidification-induced uncoupling when tested by the one-step acidification protocol.

#### Amino acids in regions 261–300 and 374–382 form the binding particle for pH gating

Previous results from our laboratory have shown that coexpression of mRNA coding exclusively for the carboxyl terminal domain (i.e., residues 259 to 382) rescues the pH sensitivity of M257 channels (Morley et al., 1996). We have therefore postulated that pH gating results from an intramolecular interaction between the carboxyl terminal (acting as a binding particle) and a separate region of the Cx molecule, acting as a receptor for the particle. We have now determined whether the ability of the carboxyl terminal domain to function as a gating particle is affected by deletion of residues in the 261–300 and the 374–382 regions.

Fig. 9, A and B, shows the results. As in the case of the data presented in Fig. 8, the plots represent the average value of  $G_j$  (normalized to  $G_j \text{ max}$ ) recorded at a given  $\text{pH}_i$ . As previously demonstrated (Liu et al., 1993; Morley et al., 1996), truncation of the carboxyl terminal at amino acid 257 led to a lack of pH sensitivity for  $\text{pH}_i$  values higher than 6.35 (Fig. 9 A, open circles). Coexpression of the carboxyl terminal domain (i.e., amino acids 259–382) together with mRNA coding for M257 rescued the pH sensitivity of the otherwise pH-insensitive channel (Fig. 9 B, grey circles; data reproduced from Morley et al., 1996). However, rescue of pH sensitivity by coexpression of the carboxyl terminal domain was prevented when segments 281–300 and 374–382 were deleted from the sequence (data M257 +  $\mu\text{CT}$ ; open squares in Fig. 9 B). The latter results could not be explained by a lack of translation of the mutant carboxyl terminal transcript. Indeed, the immunoblot presented in Fig. 9 C shows that similar amounts of both the full-length carboxyl terminal domain protein (lane labeled CT) and its mutant version (lane labeled  $\mu\text{CT}$ ) were recovered from oocytes previously injected with the corresponding mRNAs. These results confirm that the car-



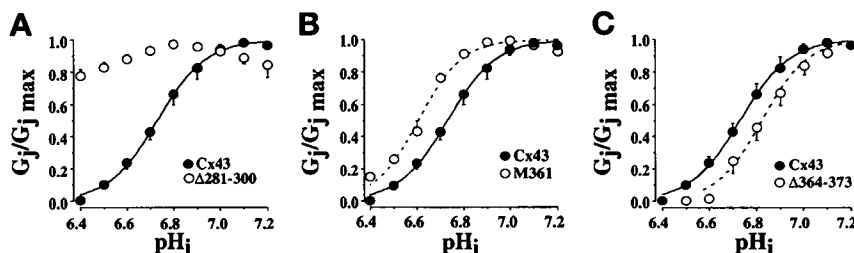


**FIGURE 8** Junctional conductance ( $G_j$ ; normalized to  $G_{j \max}$ ) as a function of intracellular pH ( $\text{pH}_i$ ). As opposed to those experiments presented in Figs. 2–7, in this case  $\text{pH}_i$  was recorded simultaneously with  $G_j$ , and the two variables were directly correlated. For these experiments, intracellular acidification was induced by superfusion of a bicarbonate-buffered solution gassed with increasing concentrations of  $\text{CO}_2$  (see Materials and Methods; see also Morley et al., 1996, for further details). Intracellular pH was measured by the emission fluorescence of the proton-sensitive dye, dextran-SNARF. In all panels, the closed circles and continuous line depict data from oocytes expressing wild-type Cx43. Five of a total of 11 experiments summarized in this figure have been reported previously (Morley et al., 1996). Values for  $\text{pK}_a$  (i.e.,  $\text{pH}_i$  that corresponds to 50% of  $G_{j \max}$ ) and the Hill coefficient were estimated for each experiment. The average  $\text{pK}_a$  recorded from Cx43-expressing oocytes was  $6.73 \pm 0.067$ , and the average Hill coefficient was  $4.85 \pm 0.30$  ( $n = 11$ ; mean  $\pm$  SEM). Average  $G_j$  in control was  $7.06 \pm 2.60 \mu\text{S}$ . **A**, Data obtained from oocytes expressing either  $\Delta 281\text{--}300$  ( $G_j$  control =  $9.91 \pm 1.71 \mu\text{S}$ ;  $n = 7$ ), M361 (**B**;  $G_j$  control =  $1.43 \pm 0.29 \mu\text{S}$ ;  $n = 6$ ) or  $\Delta 364\text{--}373$  (**C**;  $G_j$  control =  $7.41 \pm 2.04 \mu\text{S}$ ;  $n = 7$ ). Clearly, deletion of residues 281–300 or 361–382 significantly impaired pH sensitivity. On the other hand, pH sensitivity of Cx43 was not affected if the serine-rich region 364–373 was deleted from the sequence.

boxyl terminal acts as a binding particle for pH gating; the data also show that the results presented in Figs. 3 to 8 are consequent to the alteration of the gating particle structure. Finally, the data indicate that amino acids in regions 281–300 and 374–382 are essential components of the pH gating particle.

### Regions 261–300 and 374–382 are interdependent

The results presented so far show that there are two regions within the pH gating particle of Cx43 that are involved in acidification-induced closure of gap junctional channels. Additional experiments allowed us to demonstrate that the two pH-relevant regions are functionally related. Fig. 10 shows the pH sensitivity recorded from oocytes expressing mutant D379N (grey triangles). Data obtained from oocytes expressing Cx43 (solid circles, continuous line) or M361 (open circles, dotted line) are depicted for comparison. Clearly, substitution of aspartate 379 for its amide impaired pH sensitivity beyond the level observed after deletion of the entire 361–382 region. Similar results were obtained after replacing serine 364 with a proline (see below). These data show that the two regions of the carboxyl terminal that are necessary for normal pH gating are not completely independent of one another. Indeed, whereas region 261–300 can act to maintain some degree of pH sensitivity in the absence of amino acids 361–382, proper mutations of amino acid 379 (or 364; see below) can completely prevent the function of region 261–300, so that the resulting channel protein is not susceptible to acidification-induced uncoupling within the pH range tested.

### Mutation S364P prevents pH gating: is pH gating important for normal cardiogenesis?

The results presented in this paper show that point mutations in the carboxyl end can drastically alter the chemical

regulation of intercellular communication. Interestingly Britz-Cunningham et al. (1995) have shown that point mutations in the carboxyl end of Cx43 are associated with severe cardiac malformations in humans. These authors have proposed that the observed cardiac malformations may be the consequence (at least in part) of changes in the phosphorylation state of the protein. We decided to test whether substitution of serine 364 for proline, a mutation commonly found in the cases studied by Britz-Cunningham et al. (1995), would also affect the pH gating of Cx43. Results are shown in Fig. 11. Clearly, this mutation prevented pH regulation of Cx43 within the range of pH values tested. The lack of pH sensitivity seems to be unrelated to the absence of serine 364; indeed, deletion of the entire 364–373 region had no effect on pH regulation (see Fig. 8). Rather, the results are better explained by the possible modifications that the presence of a proline in that position could cause in the structure of the pH gating particle. Although highly premature, it is tempting to speculate that  $\text{pH}_i$  constitutes one of the signaling mechanisms that regulate intercellular coupling during cardiac morphogenesis; such a regulatory mechanism may then be disrupted as a consequence of the S364P mutation. Moreover, we propose that the particle receptor mechanism may be common to several regulatory pathways (including phosphorylation). In such a system, the particle-receptor recognition process may be essential for the normal function and development of the human heart.

### CONCLUSIONS

In conclusion, we have used site-directed mutagenesis and the oocyte expression system to survey the effect of different mutations of the carboxyl terminal domain on the susceptibility to acidification-induced uncoupling of Cx43 channels. The results show that two regions, one located between positions 261 and 300 and the other between res-

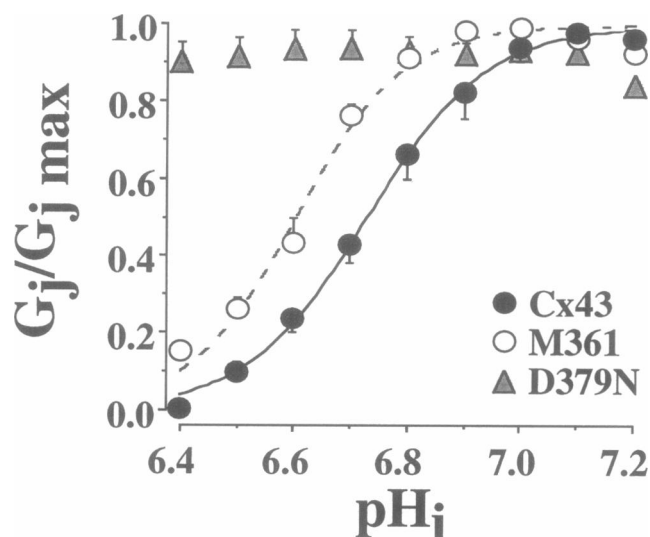
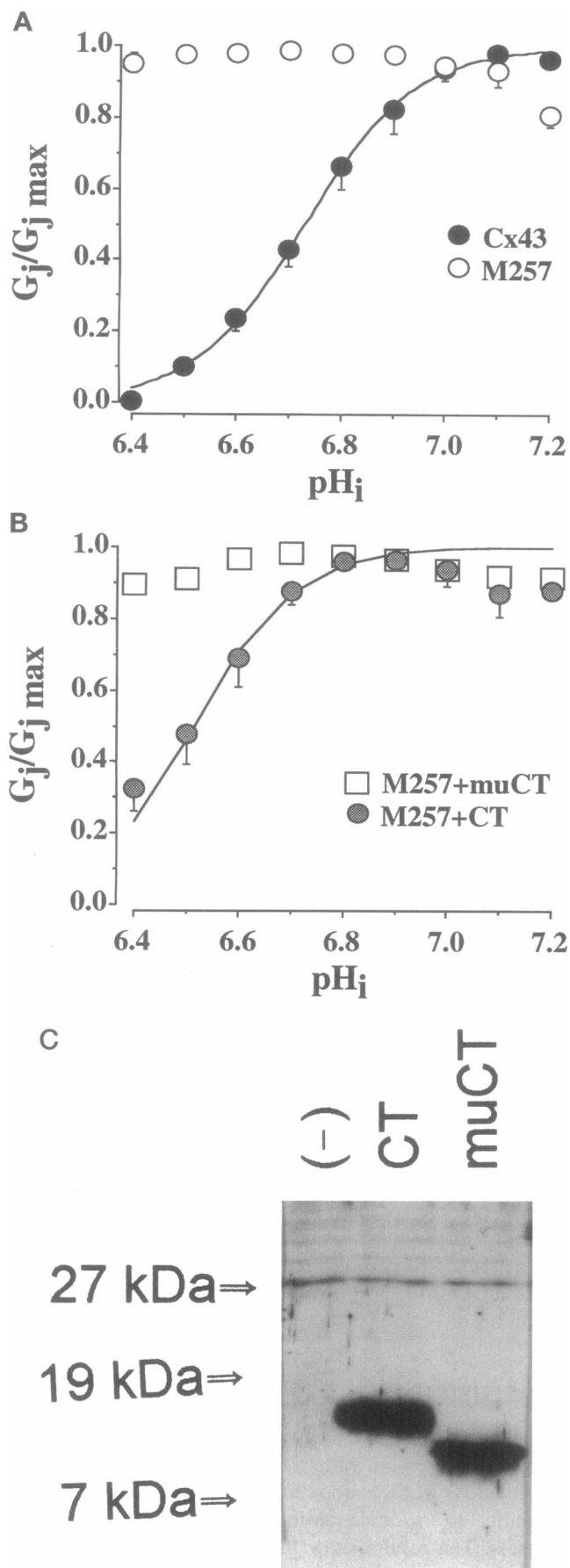


FIGURE 10 pH sensitivity of wild-type Cx43 channels (●, continuous line) and of a mutant of Cx43 where aspartate 379 was replaced for asparagine (data labeled D379N; ○,  $G_j$  control =  $4.37 \pm 2.05 \mu\text{S}$ ;  $n = 7$ ). The data show that a proper point mutation at amino acid 379 significantly impaired pH sensitivity of the Cx43 gap junction channels.

idues 374 and 382, are important for pH regulation. The regions are interdependent and may form one coordinated binding particle. We have proposed that upon acidification, this particle interacts with a separate region of the protein (acting as a receptor) to bring about the closure of the channel. A particle-receptor mechanism may be a common pathway for the chemical regulation of intercellular communication in Cx43-expressing cells. The latter may have

FIGURE 9 (A and B) Junctional conductance ( $G_j$ ; normalized to  $G_j \text{ max}$ ) as a function of intracellular pH ( $\text{pH}_i$ ). A is modified from figure 4 of Morley et al. (1996). Note that the curve for the pH sensitivity of Cx43 has been updated to include recent experiments (see legend of Fig. 8 for details). In A and B, symbols represent average data ( $\pm$ SEM) recorded from oocyte pairs injected with the following transcripts: Cx43 (●;  $n = 11$ ), M257 (○;  $n = 6$ ), M257 together with mRNA coding for amino acids 259–382 of Cx43 (labeled M257 + CT; ●;  $n = 6$ ) and M257 coexpressed with mRNA coding for amino acids 259–280 and 301–373 of Cx43 (i.e., a transcript of the CT domain, but missing regions 281–300 and 374–382; labeled M257 + mu CT; □;  $n = 8$ ). The following amounts of RNA were injected: Cx43, 30 ng/oocyte; M257, 30 ng/oocyte; CT, 0.6 ng/oocyte; mu CT, 0.6 ng/oocyte. The data show that recovery of the pH sensitivity of M257 by coexpression of the carboxyl terminal domain is prevented when amino acids 281–300 and 374–382 are missing from the sequence. (C) Immunoblot of the carboxyl terminal domain of Cx43 from oocytes injected with mRNA (0.6 ng/oocyte) for either the carboxyl terminal domain (amino acids 259–382; lane labeled CT) or the mutant carboxyl terminal domain missing amino acids 281–300 and 374–382 (lane labeled mu CT). Lane labeled (–) corresponds to uninjected oocytes. Molecular weight markers are denoted at the left. Oocytes were injected 29 h before being lysed; the protocol for oocyte injection and stripping was the same as that used for electrophysiological recordings. The CT protein (wild-type or mutant) was detected using a polyclonal anti-Cx43 antisera (Zymed, Inc). The data show that the injected mRNAs were translated into proteins of the expected size, and that the two transcripts were translated with similar efficiency.

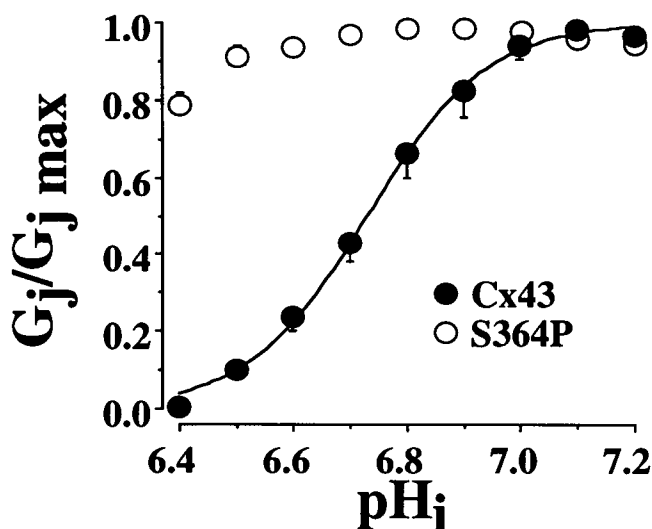


FIGURE 11 pH sensitivity of wild-type Cx43 channels (●, continuous line) and of a mutant of Cx43 where serine 364 was substituted for proline (data labeled S364P; ○,  $G_j$  control =  $10.8 \pm 1.2$ ;  $n = 9$ ). Mutation S364P has been found in some clinical cases of viscerotaxial heterotaxia (a major cardiac malformation associated with problems of laterality; Britz-Cunningham et al., 1995). The data show that this mutation can drastically alter pH-induced regulation of macroscopic gap junctional conductance.

important implications for understanding clinical syndromes associated with point mutations in the carboxyl end of Cx43.

These data constitute an initial step toward the characterization of the structural bases for particle-receptor interactions that lead to acidification-induced uncoupling of cells expressing Cx43.

The authors wish to thank Dr. Jose Jalife for his advice and support throughout the project. We also thank Ms. Kathleen Stergiopoulos for her critical reading of the manuscript. The technical assistance of Christine McElwain, Christine Kapuscinski, and Anne Caron, and the secretarial skills of Mrs. LaVerne Gilbert are greatly appreciated.

This work was supported by grants PO1-HL39707 and RO1-HL52812 from the National Institutes of Health, Heart, Lung and Blood Institute, and by a NASPE Fellowship to J.F.E.-V. Mario Delmar is an Established Investigator of the American Heart Association.

## REFERENCES

Adzhubei, A. A., and M. J. E. Sternberg. 1993. Left-handed polyproline II helices commonly occur in globular proteins. *J. Mol. Biol.* 229:472–493.

Barrio, L. C., T. Suchyna, T. Bargiello, L. X. Xu, R. S. Roginski, M. V. L. Bennett, and B. J. Nicholson. 1991. Gap junctions formed by connexins 26 and 32 alone and in combination are differently affected by applied voltage. *Proc. Natl. Acad. Sci. USA.* 88:8410–8414.

Bennett, M. V. L., L. C. Barrio, T. A. Bargiello, D. C. Spray, E. Hertzberg, and J. C. Saez. 1991. Gap junctions: new tools, new answers, new questions. *Neuron.* 6:305–320.

Bennett, M. V. L., and V. K. Verselis. 1992. Biophysics of gap junctions. *Semin. Cell Biol.* 3:29–47.

Bennett, M. V. L., R. L. Verselis, R. L. White, and D. C. Spray. 1988. Gap junctional conductance: gating. In *Gap Junctions*. E. L. Hertzberg and R. G. Johnson, editors. Alan R. Liss, New York. 287–304.

Bennett, M. V. L., X. Zheng, and M. L. Sogin. 1995. The connexin family tree. In *Intercellular Communication through Gap Junctions*. Y. Kanno, K. Kataoka, Y. Shiba, Y. Shibata, and T. Shimazu, editors. Elsevier, Amsterdam. 3–8.

Beyer, E. C., D. L. Paul, and D. A. Goodenough. 1987. connexin43: a protein from rat heart homologous to a gap junction protein from liver. *J. Cell Biol.* 105:2621–2629.

Britz-Cunningham, S. H., M. M. Shah, C. W. Zuppan, and W. H. Fletcher. 1995. Mutations of the connexin43 gap-junction gene in patients with heart malformations and defects of laterality. *N. Engl. J. Med.* 332:1323–1329.

Bruzzone, R., T. W. White, and D. L. Paul. 1994. Expression of chimeric connexins reveals new properties of the formation and gating behavior of gap junction channels. *J. Cell Sci.* 107:955–967.

Cohen, G. B., R. Ren, and D. Baltimore. 1995. Modular binding domains in signal transduction proteins. *Cell.* 80:237–248.

Creighton, T. E. 1993. *Proteins: Structures and Molecular Properties*. W. H. Freeman, New York.

Dahl, E., E. Winterhager, O. Traub, A. Butterweck, B. Reuss, and K. Willecke. 1995. Expression pattern of different connexins in comparison with communication compartments during early mouse development. In *Intercellular Communication through Gap Junctions*. Y. Kanno, K. Kataoka, Y. Shiba, Y. Shibata, and T. Shimazu, editors. Elsevier, Amsterdam. 21–25.

Dahl, G., R. Werner, E. Levine, and C. Rabadan-Diehl. 1992. Mutational analysis of gap junction formation. *Biophys. J.* 62:172–180.

Delmar, M., S. Liu, G. E. Morley, J. F. Ek, J. M. B. Anumonwo, and S. M. Taffet. 1994. Toward a molecular model for the pH regulation of intercellular communication in the heart. In *Cardiac Electrophysiology. From Cell to Bedside*. D. P. Zipes and J. Jalife, editors. W. B. Saunders, Philadelphia. In press.

Dumont, J. N. 1972. Oogenesis in *Xenopus laevis* (Daudin). I. Stages of oocyte development in laboratory maintained animals. *J. Morphol.* 136:153–180.

Ek, J. F., M. Delmar, R. Perzova, and S. M. Taffet. 1994. Role of histidine 95 on the pH gating of the cardiac gap junction protein connexin43. *Circ. Res.* 74:1058–1064.

Goldberg, S., and A. F. Lau. 1993. Dynamics of connexin43 phosphorylation in pp<sup>60v-src</sup>-transformed cells. *Biochem. J.* 295:735–742.

Hoshi, T., W. N. Zagotta, and R. W. Aldrich. 1990. Biophysical and molecular mechanisms of Shaker potassium channel inactivation. *Science.* 250:533–538.

Kanno, Y., K. Kataoka, Y. Shiba, Y. Shibata, and T. Shimazu. 1995. *Intercellular Communication through Gap Junctions*. Elsevier, Amsterdam.

Kumar, N. M., and N. B. Gilula. 1992. Molecular biology and genetics of gap junction channels. *Semin. Cell Biol.* 3:3–16.

Lim, W. A., F. M. Richards, and R. O. Fox. 1994. Structural determinants of peptide-binding orientation and of sequence specificity in SH3 domains. *Nature.* 372:375–379.

Lins, L., and R. Brasseur. 1995. The hydrophobic effect in protein folding. *FASEB J.* 9:535–540.

Liu, S., S. Taffet, L. Stoner, M. Delmar, M. L. Vallano, and J. Jalife. 1993. A structural basis for the unequal sensitivity of the major cardiac and liver gap junctions to intracellular acidification: the carboxyl tail length. *Biophys. J.* 64:1422–1433.

Morley, G. E., S. M. Taffet, and M. Delmar. 1996. Intramolecular interactions mediate pH regulation of connexin43 channels. *Biophys. J.* 70:1294–1302.

Pressler, M. 1989. Intracellular pH and cell-to-cell transmission in sheep Purkinje fibers. *Biophys. J.* 55:53–65.

Rosinski, C., and B. J. Nicholson. 1994. Determination of disulfide bond patterns in the extracellular docking domains of gap junctions. *Mol. Biol. Cell.* 5:198a.

Spray, D. C., A. L. Harris, and M. V. L. Bennett. 1981. Equilibrium properties of a voltage-dependent junctional conductance. *J. Gen. Physiol.* 77:77–93.

Stauffer, K. A., and N. Unwin. 1992. Structure of gap junction channels. *Semin. Cell Biol.* 3:17–20.

- Suchyna, T. M., L. Xian-Xu, F. Gao, C. R. Fournier, and B. J. Nicholson. 1993. Identification of a proline residue as a transduction element involved in voltage gating of gap junctions. *Nature*. 365:847-849.
- Swenson, K. I., J. R. Jordan, E. C. Beyer, and D. L. Paul. 1989. Formation of gap junctions by expression of connexins in *Xenopus* oocyte pairs. *Cell*. 57:145-155.
- Toro, L., M. Ottolia, E. Stefani, and R. Latorre. 1994. Structural determinants in the interaction of Shaker inactivating peptide and a  $\text{Ca}^{2+}$ -activated  $\text{K}^+$  channel. *Biochemistry*. 33:7220-7228.
- Vandeyar, M. A., M. P. Weiner, C. J. Hutton, and C. A. Batt. 1988. A simple and rapid method for the selection of oligodeoxynucleotide-dictated mutants. *Gene*. 65:129-133.
- Warn-Cramer, B. J., P. D. Lampe, W. E. Kurata, M. Y. Kanemitsu, L. W. M. Loo, W. Eckhart, and A. F. Lau. 1996. Characterization of the mitogen-activated protein kinase phosphorylation sites on the Connexin-43 gap junction protein. *J. Biol. Chem.* 271:3779-3786.
- Werner, R., E. Levine, C. Rabadan-Diehl, and G. Dahl. 1991. Gating properties of connexin32 cell-cell channels and their mutants expressed in *Xenopus* oocytes. *Proc. R. Soc. Lond.* 243:5-11.
- White, T. W., R. Bruzzone, S. Wolfram, D. L. Paul, and D. A. Goodenough. 1994. Selective interactions among the multiple connexin proteins expressed in the vertebrate lens: the second extracellular domain is a determinant of compatibility between connexins. *J. Cell Biol.* 125:879-892.
- White, T. W., D. L. Paul, D. A. Goodenough, and R. Bruzzone. 1995. Functional analysis of selective interactions among rodent connexins. *Mol. Biol. Cell*. 6:459-470.
- Williamson, M. P. 1994. The structure and function of proline-rich regions in proteins. *Biochem. J.* 297:249-260.
- Yu, H., J. K. Chen, S. Feng, D. C. Dalgarno, A. W. Brauer, and S. L. Schreiber. 1994. Structural basis for the binding of proline-rich peptides to SH3 domains. *Cell*. 76:933-945.